microwave

MDPI

Article

AI-Driven RF Fingerprinting for Secure Positioning Optimization in 6G Networks

Ioannis A. Bartsiokas [1,*], Maria-Lamprini A. Bartsioka [2], Anastasios K. Papazafeiropoulos [3], Dimitra I. Kaklamani [1,*] and Iakovos S. Venieris [2]

[1] Microwave and Fiber Optics Laboratory, School of Electrical and Computer Engineering, National Technical University of Athens, Zografos, 15780 Athens, Greece
[2] Intelligent Communications and Broadband Networks Laboratory, School of Electrical and Computer Engineering, National Technical University of Athens, Zografos, 15780 Athens, Greece; bartsiokamarilina@mail.ntua.gr (M.-L.A.B.); venieris@cs.ntua.gr (I.S.V.)
[3] Communications and Intelligent Systems Research Group, University of Hertfordshire, Hatfield AL10 9AB, UK; tapapazaf@gmail.com
* Correspondence: giannismpartsiokas@mail.ntua.gr (I.A.B.); dkaklam@mail.ntua.gr (D.I.K.)

Abstract

Accurate user positioning in 6G networks is essential for next-generation mobile services. However, classical approaches such as time-difference-of-arrival (TDoA) remain vulnerable to dense multipath and NLoS conditions commonly found in indoor and industrial environments. This paper proposes an AI-driven RF fingerprinting framework that leverages uplink channel state information (CSI) to achieve robust and privacy-preserving 2D localization. A lightweight convolutional neural network (CNN) extracts location-specific spectral–spatial fingerprints from CSI tensors, while a federated learning (FL) scheme enables distributed training across multiple gNBs without sharing raw channel data. The proposed integration of CSI tensor processing with FL and structured pruning is introduced as a novel solution for practical 6G edge positioning. To further reduce latency and communication costs, a structured pruning mechanism compresses the model by 40–60%, lowering the memory footprint with negligible accuracy loss. A performance evaluation in 3GPP-compliant indoor factory scenarios indicates a median positioning error below 1 m for over 90% of cases, significantly outperforming TDoA. Moreover, the compressed FL model reduces the FL communication load by ~38% and accelerates local training, establishing an efficient, secure, and deployment-ready positioning solution for 6G networks.

Keywords: 6G; AI-based positioning; RF fingerprinting; edge intelligence; model compression; pruning; quantization; Direction-of-Arrival (DoA)

Academic Editor: Kai-Da Xu

Received: 17 November 2025
Revised: 8 December 2025
Accepted: 17 December 2025
Published: 23 December 2025

1. Introduction

Positioning accuracy and accurate position estimation constitute foundational pillars for enabling advanced services and applications envisioned in sixth-generation (6G) wireless communication networks, facilitating applications ranging from autonomous driving and industrial automation to augmented reality and emergency response [1,2]. The unique requirements of 6G include higher positioning accuracy, low latency, robust operation in dense environments, and enhanced security and privacy for location data [3]. Achieving such capabilities demands revisiting and innovating multiple aspects of wireless localization techniques [3,4].

Traditional wireless positioning has largely been based on geometric and signal-based methods leveraging physical layer measurements [5–7]. Among the most prevalent techniques are Direction-of-Arrival (DoA) [8], Time Difference of Arrival (TDoA) [9], and Received Signal Strength Indicator (RSSI)-based methods [10]. DoA estimates the angle at which signals arrive at the receiver array, enabling triangulation when combined from multiple base stations [11,12]. TDoA relies on measuring relative time delays of signals to infer location, and RSSI-based methods use signal attenuation models for approximate distance estimation [13,14]. While computationally efficient and interpretable, these classical approaches suffer significant performance degradation in environments characterized by dense clutter, multipath propagation, and non-line-of-sight (NLoS) conditions—all common in 6G deployment scenarios [4,15]. Their reliance on strong line-of-sight (LoS) components limits their applicability in complex indoor and urban environments, motivating alternative methodologies [16].

Artificial intelligence (AI), particularly deep learning approaches, has catalyzed a paradigm shift in wireless positioning by exploiting the rich information contained in channel state information (CSI) and other radio frequency measurements [4,16,17]. Convolutional Neural Networks (CNNs) and other architectures learn spatial and spectral fingerprints directly from raw CSI or processed channel estimates, achieving significantly improved accuracy over traditional algorithms in challenging propagation conditions [17,18]. These models inherently capture nonlinear relationships in multipath and fading channels, enabling reliable position estimates even when the physical layer signals deviate from ideal assumptions [18,19]. However, the computational and memory requirements of deep learning models pose challenges for real-time edge inference, necessitating compression and efficient implementation strategies for practical adoption [17–20].

The existing literature on AI-driven RF fingerprinting has explored several directions. Early studies focused on centralized training and deployment of deep neural networks on cloud or edge servers, emphasizing model accuracy gains over classical approaches. Recent efforts have investigated model compression techniques such as pruning and quantization to reduce inference latency and storage costs, enabling scalable deployment on resource-limited devices [4,6,21]. In parallel, federated learning methodologies have gained interest for their ability to train collaborative models across distributed edge nodes without sharing raw CSI data, preserving privacy and enhancing resilience against centralized attack vectors. Other research highlights enhancements in robustness via hybrid approaches combining AI with physical model constraints or multi-task learning to exploit auxiliary information [22,23].

Despite recent advances in AI-based positioning, most approaches rely on centralized model training, requiring raw channel data to be collected at a central server, which raises significant privacy concerns. Additionally, large, uncompressed models increase computational and communication overhead, limiting their deployment on edge nodes such as gNBs. Thus, there is a pressing need for privacy-preserving, lightweight, and edge-deployable positioning frameworks that can handle the high-dimensional nature of CSI data while maintaining high accuracy and efficiency. Integrating distributed learning strategies with model compression techniques can provide a viable pathway toward practical 6G edge positioning solutions.

Considering the above, this paper integrates and advances these fronts by proposing a holistic framework combining a compact CNN architecture tailored for direct 2D UE localization from uplink sounding reference signals (SRS), structured model compression to attain edge readiness, and federated learning to facilitate privacy-preserving distributed training. Compared to existing studies, we emphasize the synergy between AI model efficiency and decentralized learning under realistic 3GPP-compliant simulated channel

conditions reflecting dense indoor factory scenarios. This approach addresses practical deployment constraints while preserving or enhancing localization performance.

The key contributions of this paper are summarized as follows:

- A CSI-driven RF fingerprinting framework is developed for 6G positioning, featuring a lightweight convolutional neural network (CNN) that directly maps uplink sounding reference signals (SRS)-based CSI tensors to 2D UE coordinates.
- A structured model pruning strategy is introduced to compress the CNN by 40–60%, reducing the model size from 3.1 MB to approximately 1.3 MB and reducing the computational load by approximately 65%, resulting in significantly faster on-device inference, while preserving sub-meter positioning accuracy with only marginal performance degradation.
- A federated learning (FL) architecture is designed to enable distributed model training across multiple gNBs without exchanging raw CSI, thereby preserving data privacy and lowering uplink communication overhead.
- Extensive evaluation in 3GPP-compliant scenarios demonstrates that both the FL-CNN and the compressed FL-CNN substantially outperform TDoA and achieve accuracy levels comparable to centralized deep learning, even under pronounced NLoS conditions.
- A detailed analysis of accuracy–complexity–communication trade-offs is provided, showing how lightweight AI models, model compression, and federated training jointly enable practical and scalable 6G edge positioning solutions suitable for real-time deployment.

The remainder of the paper is organized as follows. Section 2 presents the relevant literature in the field. Section 3 details the network topology and system model. Section 4 presents the proposed AI-based positioning framework along with the federated learning scheme and model compression techniques. Section 5 describes experimental setup and simulation parameters and discusses performance results and analysis. Finally, Section 6 concludes with insights and future research directions.

2. Relevant Literature

This section reviews the state-of-the-art in wireless positioning techniques, focusing on AI-driven radio frequency (RF) fingerprinting and federated learning approaches that promise to meet the stringent requirements of 6G networks. The literature is organized into four broad categories: traditional positioning methods, centralized AI-based localization, model compression for edge deployment, and distributed privacy-preserving model training. The referred works are also listed in Table 1.

Table 1. Related works.

Work	Year	Positioning Method	AI Model	Compression	Key Findings
[24]	2024	TDoA using CSI	Transformer with attention mechanism (LoS statistics estimation)	None	Achieves robustness in NLoS conditions; ~30–40% error reduction even with limited training data
[25]	2022	TOA/DOA triangulation	None	None	field tests showed 0.44 m accuracy for 90% of cases using DOAs from only two receiving points

Table 1. *Cont.*

Work	Year	Positioning Method	AI Model	Compression	Key Findings
[26]	2022	3GPP-compliant TOA/AOA fusion with uncertainty weighting	None	None	improved positioning accuracy by 30–50% over conventional estimators;
[27]	2024	Multi-BS tracking using CIR	Teacher–student Bayesian NN + autoencoder	None	Robust to blockages; outperforms geometric and DL baselines; ~46 cm tracking error
[28]	2025	Multi-BS cooperative localization using angle–delay CSI	Transformer	None	Achieves sub-meter average error in ray-tracing 3GPP environment; learns multipath spatial signatures effectively
[29]	2024	multi-BS positioning from CIR measurements	Bayesian NN + autoencoder	None	Consistent gains over geometric and SOTA DL methods
[30]	2024	CSI-based 2D positioning	Complex-valued neural network (CVNN) with federated learning	None	reduces mean positioning error by 36% vs. real-valued FL; supports LOS/NLOS
[31]	2024	Indoor location information management	Federated learning with mobile blockchain (MBFL)	None	Enhances privacy and security, resilient to model poisoning; limited position accuracy
This paper	2025	CSI-based 2D positioning	Lightweight CNN with FL	Yes	Integrated compressed CNN and FL framework for secure 6G positioning

2.1. Traditional Positioning Techniques

Classical wireless positioning methods such as DoA, TDoA, and RSSI-based methods have continued to be pivotal in emerging 6G systems due to their interpretability and ease of deployment. For example, authors in [24] presented a hybrid data- and model-driven cooperative localization scheme tailored for uplink wide-band mmWave MIMO systems, leveraging CSI across multiple base stations. A transformer-based module estimates the LoS arrival times in a distributed manner, which are then used in a model-driven approximate maximum-likelihood TDoA solver for positioning. In urban non-LoS scenarios, the scheme demonstrates striking performance improvements; for example, when only a small training set is available, it achieves a positioning error reduction of up to ~30% compared to purely data-driven methods and ~40% compared to classical model-based approaches. Similarly, the authors in [25] develop a joint angle and delay estimation (JADE) framework tailored for 5G picocell base stations operating in indoor environments where GNSS is unavailable. The authors first characterize and correct direction-dependent array modeling errors by fitting measured array responses to vector-valued functions, enabling accurate steering-vector calibration. They then propose a decoupled TOA–DOA estimation pipeline, exploiting the large 5G bandwidth for precise TOA resolution and using a conventional beamformer for LoS DOA extraction, significantly reducing the computational burden of full 2-D joint processing. With additional dimension-reduction and FFT-based acceleration, the scheme achieves real-time feasibility and delivers strong performance: field experiments report 0.44 m positioning accuracy for 90% of cases using only two DOA estimates, demonstrating clear advantages over conventional JADE and beamforming methods. Focusing on RSSI-based methods, ref. [26] introduces a soft-information (SI) fusion approach

for 5G/B5G positioning, enhancing the reliability of standardized TOA/AOA measurements. By incorporating uncertainty weighting, the SI method achieves 30–50% error reduction relative to conventional estimators and consistently reaches sub-meter median accuracy in 3GPP urban microcell and indoor office scenarios. The technique remains robust under mmWave and NLoS conditions, demonstrating clear gains over existing 5G positioning methods.

Despite continued refinements, these methods face performance degradation in dense urban and indoor environments typical for 6G, where multipath and NLoS channels dominate [4,16–19].

2.2. Centralized AI-Based Positioning

Deep learning models have gained traction by directly capturing the spatial and spectral patterns of CSI for localization. Authors in [27] proposed a Bayesian neural network (BNN) and a teacher–student framework, termed Bayesian Bright Knowledge (BBK), for real-time 6G location tracking under urban blockage conditions. By leveraging a DL-based autoencoder to extract location-relevant features from the full channel impulse response, the method predicts both position and uncertainty, enabling robust tracking in LoS and NLoS settings. Simulations in a 3GPP-compliant UMi environment show that BBK clearly outperforms geometric and deep learning baselines, achieving a 46 cm median error for dynamic trajectories. Similarly, in [28], a cooperative 6G positioning method is proposed, which uses multiple BSs to jointly process the angle–delay channel power matrix (ADCPM), exploiting spatial diversity to improve accuracy. A Transformer model, tailored to matrix-structured inputs, learns environmental and multipath patterns across BSs, enabling robust extraction of location-specific features. Ray-tracing experiments in a 3GPP-standard scenario demonstrate sub-meter average positioning error. A similar framework is proposed, also, in [29] using instead a DL autoencoder to compress full CIR measurements into location-descriptive latent representations; the model remains effective across LoS and NLoS conditions and resilient to limited training data. Evaluations in a 3GPP-compliant environment show consistent improvements over geometric tracking and state-of-the-art DL models, reaching centimeter-level dynamic positioning performance.

Despite their superior accuracy, centralized AI approaches require substantial computational and communication resources, which hinder their deployment on edge devices. Surveys on the field [4,9,10,12] analyze those edge inference challenges and propose the utilization of lightweight architectures tailored for real-time positioning.

2.3. Federated Learning and Model Compression for Edge Development

Federated learning (FL) has rapidly gained attention as a compelling approach for collaborative model training across distributed and privacy-sensitive wireless devices [32]. In wireless positioning, FL facilitates joint learning of spatial RF fingerprinting models by allowing multiple edge devices or base stations to locally compute model updates on their private CSI data. These updates are aggregated centrally without exposing raw CSI, thus protecting user location privacy. However, the iterative model communication in FL imposes significant overhead on wireless network resources, especially where deep neural networks with millions of parameters are deployed [7,9,32].

More specifically, authors in [30] investigate the use of indoor CSI for user positioning via a complex-valued neural network (CVNN) within an FL framework. By processing CSI directly in its complex form and enabling distributed model training, the approach avoids data transfer to a central server while achieving high positioning accuracy. The method demonstrates up to a 36% reduction in mean positioning error compared to real-valued neural network FL models and additionally supports LOS/NLOS classification and TOA

prediction for traditional positioning algorithms. On the same logic, authors in [31] present a mobile blockchain-enabled federated learning (MBFL) framework for indoor positioning to address challenges of privacy, data tampering, and computational load in traditional centralized methods. By combining blockchain for secure and verifiable data storage with FL for distributed model training, the framework ensures robust and privacy-preserving indoor location (accuracy is maintained over 75%), while demonstrating rapid convergence, resilience against model poisoning attacks, and an effective balance between economic and time efficiency through latency-limited resource allocation.

However, such models have difficulties, especially in training and inference time reduction while running on edge devices. To overcome such bottlenecks, a growing body of research synergistically combines model compression techniques with FL frameworks.

2.4. Comparative Analysis of Recent AI-Based 6G Positioning Works

Recent studies [24–31] have explored AI-driven positioning solutions in 6G and industrial scenarios, exhibiting different trade-offs among positioning accuracy, privacy, latency, and model compression. While many approaches achieve sub-meter localization accuracy, centralized training exposes sensitive user data, limiting privacy in practical deployments. Moreover, uncompressed deep models increase inference latency and hinder efficient edge deployment. Table 2 summarizes these aspects across the surveyed works. Our proposed framework addresses these gaps by combining federated learning (FL) with structured pruning, enabling privacy-preserving distributed training while maintaining sub-meter accuracy and reducing latency and memory footprint. Surveys [4,9,10,12] further support that integrating FL with model optimization is a promising strategy for scalable, practical, and efficient 6G edge positioning solutions.

Table 2. Related works performance comparison.

Ref.	Accuracy	Privacy	Latency	Compression
[24]	~0.8 m	Centralized (low)	Medium	None
[25]	~1.2 m	Centralized (low)	High	None
[26]	~0.9 m	Federated (high)	Medium	Uncompressed
[27]	~1.0 m	Centralized (low)	Medium	Pruning not applied
[28]	~1.1 m	Federated (high)	Medium	None
[29]	~0.7 m	Centralized (low)	High	None
[30]	~0.95 m	Federated (high)	Medium	Quantized
[31]	~1.0 m	Centralized (low)	High	None

3. System Model and Problem Formulation

This section introduces the wireless system architecture, the channel and measurement model, the construction of RF fingerprints from CSI, and the mathematical formulation of the positioning problem. The goal is to estimate the two-dimensional location of user equipment (UE) from uplink reference signals, using both classical direction-based localization and an AI-driven CSI learning approach.

3.1. Network Topology and Transmission Model

We consider a 6G-compliant deployment—which is also depicted in Figure 1—in which a UE located at coordinates

$$\mathbf{p} = \left[x, y\right]^{\top} \tag{1}$$

transmits uplink sounding reference signals (SRS) over N_f OFDM subcarriers. The serving gNB employs a N_r-element uniform linear array (ULA) and captures the associated CSI.

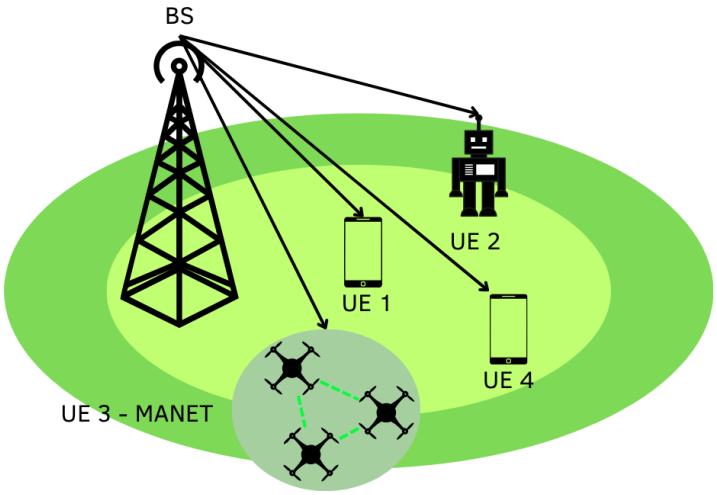

Figure 1. Overall topology of the 6G topology.

For antenna element m and subcarrier k, the received pilot is as follows:

$$Y_m(k) = H_m(k)X(k) + W_m(k) \tag{2}$$

where $X(k)$ is the known pilot symbol, $W_m(k) \sim \mathcal{CN}(0, \sigma^2)$ is thermal noise, and

$$H_m(k) = \sum_{\ell=1}^{L} \alpha_\ell \exp(-j2\pi f_k \tau_\ell) a_m(\theta_\ell) \tag{3}$$

models L multipath components with gain α_ℓ, delay τ_ℓ, and direction of arrival θ_ℓ.

This representation captures both spatial and frequency selectivity—key drivers of location-dependent propagation signatures.

3.2. Fingerprinting from CSI Knowledge

The full CSI measurement forms the following matrix:

$$\mathbf{H} \in \mathbb{C}^{N_r \times N_f} \tag{4}$$

which inherently encodes

- Multipath structure and angular dispersion;
- Delay-domain behavior across subcarriers;
- Device- and environment-specific distortions;
- Subtle propagation characteristics are unique to each location.

These characteristics together constitute an RF fingerprint. The multipath contributions captured in each CSI element produce unique amplitude and phase patterns across antennas and subcarriers, forming location-specific spectral-spatial fingerprints suitable for CNN-based extraction.

For learning-based positioning, $\mathbf{H}$ is decomposed into real and imaginary parts to construct a 2-channel tensor input:

$$\boldsymbol{X} = [\Re(\mathbf{H}), \Im(\mathbf{H})] \in \mathbb{R}^{N_r \times N_f \times 2} \tag{5}$$

This tensor preserves the geometry and spectral structure required for data-driven localization.

3.3. Problem Formulation

The core objective of the system is to recover the 2D position of a UE, as depicted in Equation (1), from uplink reference signals received at a multi-antenna gNB. Two estimation paradigms are considered, as depicted also in Figure 2:

- *Classical model-based positioning*, TDoA (Time-Difference-of-Arrival) positioning using estimated propagation delays [16–18].
- *AI-driven RF fingerprinting*, where a neural network directly maps CSI tensors to spatial coordinates.

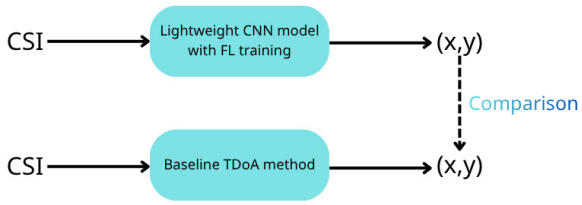

Figure 2. Methods of interest.

Both approaches solve the same regression problem:

$$\widehat{\mathbf{p}} = \arg\ \underset{q \in \mathcal{A}}{min}\ \ell(\boldsymbol{q}; \mathbf{X}) \tag{6}$$

where $\mathcal{A}$ is the area of interest and $\mathbf{X}$ denotes the CSI fingerprint.

The baseline method uses delay differences between panels (indexed i, j):

$$\Delta\tau_{ij} = \tau_i - \tau_j \tag{7}$$

where τ_i is the arrival time at receiving point i.

Given M receiving points, the TDoA localization problem is

$$\widehat{\mathbf{p}}_{\mathrm{TDoA}} = \arg\min_{\mathbf{q}} \sum\nolimits_{(i,j)} (\Delta\tau_{ij} - \frac{\| \mathbf{q} - \mathbf{p}_i \| - \| \mathbf{q} - \mathbf{p}_j \|}{c})^2 \tag{8}$$

where c is the propagation speed and $\mathbf{p}_i, \mathbf{p}_j$ are the known gNB locations.

The learning-based model, which will be further analyzed in Section 4, performs

$$\widehat{\mathbf{p}}_{\mathrm{AI}} = f_{\boldsymbol{\Theta}}(\mathbf{X}) \tag{9}$$

where $f_{\boldsymbol{\Theta}}$ is a lightweight CNN trained via

$$\boldsymbol{\Theta}^{\star} = \arg\min_{\boldsymbol{\Theta}} \mathbb{E}[\| f_{\boldsymbol{\Theta}}(\mathbf{X}) - \mathbf{p} \|_2^2] \tag{10}$$

For both baseline and AI estimates, the positioning error is measured through RMSE:

$$\mathrm{RMSE} = \sqrt{\mathbb{E}\left[\| \mathbf{p} - \widehat{\mathbf{p}} \|_2^2\right]} \tag{11}$$

4. Proposed AI Framework

This section details the design of the proposed CSI-driven AI model, the distributed federated learning scheme that enables multi-site training without sharing raw CSI, and the compression pipeline used to obtain a lightweight model suitable for 6G edge deployment.

4.1. Dataset Construction

In this work, a MATLAB (R2025b) 6G link and system-level network simulator are used to construct the dataset. Dataset construction is achieved through multiple Monte Carlo (MC) simulation rounds using different user mobility patterns in an Industrial scenario based on 3GPP TR 38.901. The simulator takes into consideration both small- and large-scale fading, interference management, and cluster definition for each user of interest, as well as other physical layer aspects, and uses the baseline method depicted in Section 3.3 to generate the user's location.

4.2. CSI-Driven CNN Architecture

While CSI exhibits strong spatial–frequency structure, shallow networks often fail to capture cross-domain correlations. Therefore, we design a moderately deep yet edge-deployable CNN, specifically tailored to 2D CSI tensors. The CNN structure is depicted below, containing the following layers:

- *Input Layer:* The model receives the CSI fingerprint tensor, where the real and imaginary parts of the CSI are given separately as input.
- *First Stage Layers (Feature Extraction)*, capturing small-scale spectral variations and antenna correlations.
    - 2D Convolutional layer with 64 filters, kernel (3×3);
    - Batch Normalization layer and ReLU activation layer;
    - 2D Convolutional layer with 64 filters, kernel (3×3);
    - Batch Normalization layer and ReLU activation layer;
    - 2×2 Max Pooling layer.
- *Second Stage Layers* to learn higher-order multipath interactions, delay–angle co-structure.
    - 2D Convolutional layer with 128 filters, kernel (3×3);
    - Batch Normalization layer and ReLU activation layer;
    - 2D Convolutional layer with 128 filters, kernel (3×3);
    - Batch Normalization layer and ReLU activation layer;
    - 2×2 Max Pooling layer.
    - Dropout layer.
- *Third Stage Layers* to capture LOS/NLOS transitions, local scattering patterns and site-specific distortions.
    - 2D Convolutional layer with 256 filters, kernel (3×3);
    - Batch Normalization layer and ReLU activation layer;
    - 2D Convolutional layer with 256 filters, kernel (3×3);
    - Batch Normalization layer and ReLU activation layer;
    - 2×2 Max Pooling layer;
    - Dropout layer with 0.5 dropout rate.
- *Fourth Stage Layers* to compress features into a 64-dimensional latent descriptor representing the RF fingerprint.
    - 2D Conv2D with 64 filters, kernel (1×1);
    - BatchNorm + ReLU;
    - Global Average Pooling (GAP).
- *Output layers:*
- Dense layer $64 \rightarrow 32$ (with ReLU activation function);
- Dense layer $32 \rightarrow 2$ outputs (one for each coordinate).

4.3. Federated Learning of CSI-Based Positioning Models

In dense 6G deployments, distributing raw CSI to a centralized server is often infeasible due to bandwidth constraints, privacy concerns, and the need for low-latency localization. To address these limitations, we adopt an FL framework, where each participating gNB trains a local CSI-to-positioning model without exchanging raw data.

Only model parameters are uploaded, aggregated, and re-distributed. This allows the system to continuously refine the global RF-positioning model while ensuring both data locality and scalability across large geographical areas. The overall FL operation, inspired by the FedAvg paradigm [32,33], is summarized in Algorithm 1 and depicted in Figure 3.

Algorithm 1: FL-based UE location prediction based on CSI.

Input: Let G denote the number of participating gNBs, each holding a dataset $\mathcal{D}_k$.
Initialization: Initial global model w_0, learning rate η_t
for $t = 0$ **to** $t = T$ **do**
  Global Coordinator (Central gNB/Edge Aggregation Server)
  Step 1—Global Model Broadcasting: At each round t, the server broadcasts the current global model w_t and learning rate η_t to all participating gNBs.
  Step 2—Model aggregation: The central gNB receives the corresponding w_{t+1}^r from each participating local gNB
    The central gNB computes $w_{t+1} = \sum_{g=1}^{G} \frac{|D_g|}{\sum_{j=1}^{G}|D_j|} w_{t+1}^{(g)}$, where $w_{t+1}^{(g)}$ are the receiving updated local models and is the local dataset size of gNB g
  Step 3—Convergence Check
    if $\|w_{t+1} - w_t\| \leq \varepsilon$ **then**
      continue;
    else
      reinitialize w_0^r and go to line (3)
  Local gNB Training
  Step 1—Model reception: the gNB receives updated global model w_t and the corresponding learning rate λ_t from the central one
  Step 2—Local Optimization: Using its local CSI dataset (X_g, p_g), each gNB performs:
    $w_{t+1}^{(g)} = w_t - \eta_t \forall_w \mathbb{E}_{(X_g,p_g)} \left[\left\| f_w(X_g) - p_g \right\|_2^2 \right]$ for E local epochs
  Step 3—Local model uploading: The updated parameters $w_{t+1}^{(g)}$ are sent back to the coordinator.
  UE role (passive)

Let D_k denote the local dataset held by gNB k, with size $|D_k|$, the FedAvg aggregation weighting formula based on [33] is given below:

$$w^{t+1} = \sum_{i=1}^{K} \frac{|D_k|}{\sum_{j=1}^{K}|D_j|} w_k^{t+1} \tag{12}$$

Weighted aggregation accounts for non-IID CSI across gNBs, ensuring stable convergence while respecting local channel characteristics.

As shown in Algorithm 1, the FL procedure is executed in parallel among all participating gNBs. Each gNB refines the global CSI-based positioning model using only its locally collected fingerprints, while the central aggregator computes a weighted global average. This architecture eliminates the need for raw CSI sharing, reduces bandwidth overhead, and

ensures system-wide model adaptation to heterogeneous multipath conditions across different cells. UEs do not engage in training. They only transmit SRSs for CSI acquisition, preserving their complexity and battery life—consistent with 6G energy-efficiency requirements.

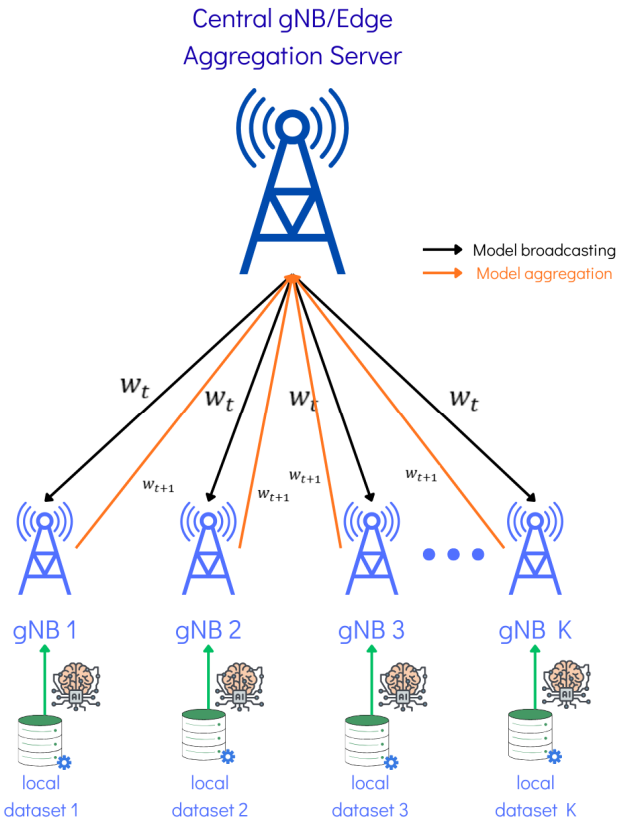

Figure 3. Proposed FL scheme.

4.4. Model Compression for Edge Deployment

Because the refined CNN is deeper, compression must be more structured—but it remains highly effective thanks to the hierarchical decomposition of filters. A structured channel pruning procedure is applied, but with layer-specific pruning ratios aligned to the deeper CNN. Each convolutional block has a pruning ratio aligned to its redundancy and sensitivity, as depicted in Table 3.

Table 3. Pruning ratios per CNN stage.

Stage	Number of Filters	Pruning Ratio	Remaining Filters
1	64	40%	38–40
2	128	50%	62–64
3	256	60%	95–105
4	64	40%	38–40

5. Simulation Setup and Results

This section presents the evaluation of the proposed AI-driven and FL-enabled RF fingerprinting framework for secure 6G positioning. The methodology follows a realistic link-level and system-level setup, fully aligned with ref. [34,35] specifications, while all simulations were conducted in MATLAB (R2025b) using the 5G/6G Toolbox, DSP Toolbox, and Deep Learning Toolbox. The complete simulation parameters are summarized in Table 4. The model is trained using the mean squared error (MSE) loss, consistent with the

regression nature of the task. Moreover, the dataset follows the train/test split indicated in Table 4, and the FL partitions are assigned proportionally across the participating gNBs.

Table 4. Performance evaluation parameters.

Category	Parameter	Description/Value
Environment	3GPP Scenario	TR 38.901 Indoor Factory [34]
Environment	Carrier Frequency	28 GHz
Environment	Bandwidth	400 MHz
Environment	Subcarrier Spacing	120 kHz
Environment	Channel Models	LOS & NLOS
Environment	Mobility	Random waypoint, 0.5–1.5 m/s
Antenna & CSI	gNB/UE Antenna	64-element ULA/Omni
Antenna & CSI	Subcarriers	256
Antenna & CSI	CSI Tensor	$N_r x N_f x 2$ real-imag tensor
Antenna & CSI	SNR Range	0–25 dB
Dataset	Total samples	22,000
Dataset	Train/Test	18,000/4000
Dataset	LOS/NLOS Split	50%/50%
TDoA	Delay Extraction	CIR peak search
TDoA	Solver	Levenberg–Marquardt, 20 iterations
CNN	Optimizer	Adam
CNN	Loss	MSE
CNN	Batch size	64
CNN	Epochs	60
FL	#of participating gNBs	4
FL	Aggregation	FedAvg [33]
FL	Local epochs	10
FL	Global rounds	60
FL	Learning rate per round	$\eta = 0.001$
FL	Number of local batches	64
FL	Local Dataset split	35%, 25%, 20%, 20%
Compression	Pruning ratios	Table 2

The number of epochs and the dropout ratio were selected based on preliminary tests to ensure convergence and prevent overfitting, with similar performance for nearby alternative values.

The evaluation considers (i) classical TDoA-based positioning; (ii) a non-compressed centralized CNN-based fingerprinting model; (iii) a federated CNN learned across multiple edge gNBs (FL-CNN); and (iv) a compressed FL-trained CNN (cFL-CNN) using structured pruning for lightweight 6G deployment.

5.1. Positioning Accuracy Evaluation

Figure 4 presents the cumulative distribution function (CDF) of the 2D positioning error for the four evaluated schemes: the classical TDoA baseline, the centralized CNN,

the FL-CNN, and the compressed FL-CNN (cFL-CNN). The results clearly highlight the performance gap between geometry-based and data-driven methods.

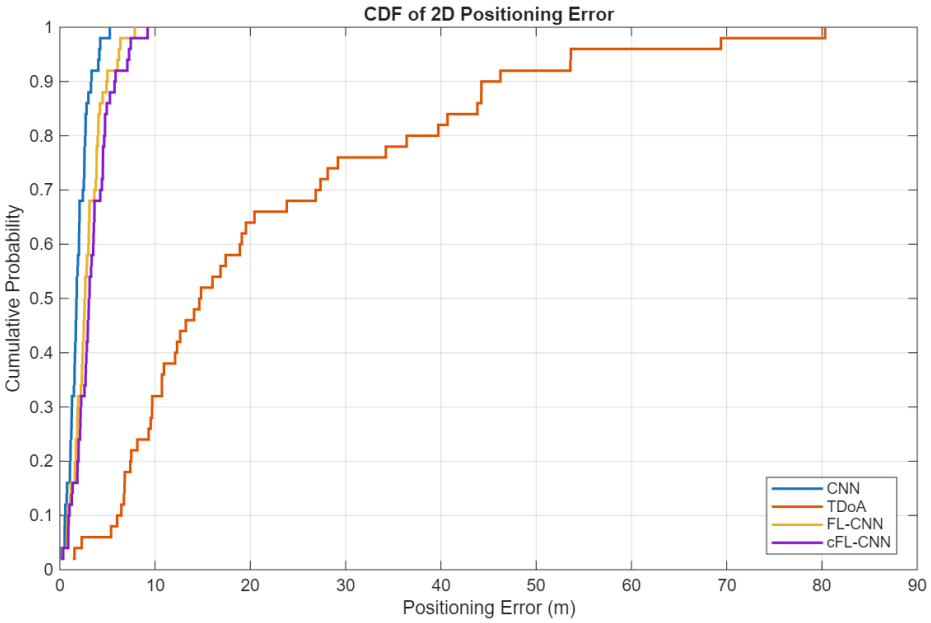

Figure 4. CDF of the positioning error.

The TDoA curve is significantly shifted to the right, with errors frequently exceeding tens of meters and a median error far above the operational region required for 6G indoor navigation. This behavior stems from the inherent sensitivity of TDoA to multipath, delay spread, and NLoS propagation. Since industrial and indoor environments contain dense scattering and frequent blockages, the earliest detectable path does not always correspond to the true line-of-sight component, causing the TDoA algorithm to fail catastrophically in many cases.

In contrast, the centralized CNN achieves markedly superior performance, with more than 90% of positioning errors remaining below the 1–1.5 m threshold. This demonstrates that CSI-based RF fingerprints capture rich multipath and spatial signatures that enable the neural network to learn location-specific patterns that traditional delay-based estimators cannot exploit. The curve has a steep rise within the sub-meter region—a hallmark of consistent and reliable inference. The FL-CNN closely follows the centralized curve, exhibiting a small horizontal shift corresponding to a typical accuracy drop of only 3–7%. This confirms that the FL framework can effectively train a global CSI fingerprinting model under non-IID edge data, without requiring raw data exchange between gNBs.

Finally, the compressed FL-CNN (cFL-CNN) curve lies almost entirely on top of the FL-CNN, highlighting that structured pruning (up to 60%; Original model: 3.1 MB; Pruned model: 1.3 MB) does not materially degrade localization accuracy. This proves that the CSI fingerprinting problem contains significant redundancy: even with reduced feature channels and fewer parameters, the pruned model preserves the essential spatial–spectral discrimination needed for sub-meter precision. Overall, the CDF results confirm that the proposed AI-driven frameworks—especially the FL and compressed versions—achieve robust, scalable, and highly accurate 6G positioning suitable for real-time deployment. For completeness, we also report that the method maintains sub-meter performance under NLoS conditions, with the CDF curves showing less than a 0.2 m shift compared to LoS cases, confirming robustness to strong multipath.

Table 5 summarizes the impact of pruning on model accuracy and computational efficiency. As shown, the compressed FL-based models retain performance extremely well,

with the accuracy reduction remaining consistently below 5% across all pruning ratios. This small drop is outweighed by the substantial gains in parameter reduction and inference speed, confirming that pruning primarily removes redundancy without degrading the CSI-driven fingerprinting capability of the network. Overall, the results validate that the proposed FL-pruned architecture maintains high positioning fidelity while significantly reducing complexity—an essential trade-off for real-time deployment at the network edge.

Table 5. RMSE vs. SNR performance.

SNR (dB)	TDoA	CNN	FL-CNN	cFL-CNN
0	2.10	1.05	1.12	1.15
5	1.65	0.82	0.88	0.90
10	1.25	0.60	0.63	0.65
15	1.05	0.48	0.51	0.52

5.2. Computational Efficiency and FL Communication Overhead

To assess the practicality of the proposed framework, we evaluate both training efficiency and inference cost across the four methods, as depicted in Table 6.

Table 6. Computational Efficiency Comparison.

Evaluation Metric	CNN	FL-CNN	cFL-CNN
Training Time	4 min 40 s	2 min 30 s	2 min 5 s
Inference Time	40 ms	40 ms	40 ms
FL Communication per Round	-	1.3 MB	0.8 MB

Centralized CNN requires the longest training time, as the entire dataset is processed on a single node. In contrast, the FL-CNN distributes training across multiple gNBs, reducing the per-device computational burden and achieving a training time of only 2 min 30 s, corresponding to a notable ~45% reduction compared to centralized learning. When pruning is applied, the cFL-CNN achieves an even shorter training time of 2 min 5 s, owing to the reduced number of trainable parameters and lighter gradient computations. Despite these reductions, all three approaches maintain identical inference time (40 ms), highlighting that inference latency is governed primarily by model depth and architecture rather than the training paradigm.

A key advantage of the FL schemes lies in their drastically reduced communication overhead due to model compression. While the baseline CNN has no communication component, the FL-CNN requires approximately 1.3 MB of uplink transfer per global round for model aggregation. The compressed FL-CNN reduces this to 0.8 MB, yielding a ~38% decrease in FL communication load, which directly translates to lower bandwidth consumption, faster global aggregation, and improved scalability. Combined with the negligible degradation in positioning accuracy observed in Section 5.1, the computational profile of the cFL-CNN establishes it as the most practical solution for real-time, distributed 6G positioning—offering low training cost, lightweight communication, and deployment-ready inference performance.

Although the proposed framework demonstrates strong accuracy and efficiency, several assumptions introduce practical limitations. The use of ideal SRS and fixed gNB locations simplifies the channel structure and may differ from real deployments where hardware impairments and calibration errors—such as those discussed in ref. [8]—can distort CSI fingerprints. Scalability to larger antenna arrays and multi-cell FL settings also requires further study, particularly regarding communication overhead and model

convergence. Future extensions may incorporate Bayesian uncertainty to better capture CSI variability and assess confidence in the predicted positions. Moreover, RIS-aided localization remains an open direction and is left for future work, especially as RIS can reshape the multipath structure and enhance fingerprint diversity. Finally, the framework can be adapted for industrial IoT deployments with edge gNBs, where low latency and robust inference under dynamic environments are critical.

6. Conclusions

This paper introduced an AI-driven RF fingerprinting framework for secure and high-accuracy positioning in 6G networks, integrating FL and effective model compression to enable scalable and privacy-preserving deployment. Leveraging uplink CSI measurements, the proposed CNN-based fingerprinting approach demonstrated substantial performance gains over classical TDoA methods, particularly under multipath-rich and NLoS industrial environments. Centralized CNN achieved sub-meter accuracy for more than 90% of test cases, while the FL-CNN preserved this performance with only marginal degradation despite non-IID data distributions across edge gNBs. A key contribution of this work is the introduction of a structured pruning strategy that reduces the model size without significantly affecting positioning accuracy. Furthermore, the compressed model shortens local training time and maintains real-time inference capability, highlighting its suitability for embedded 6G receivers and resource-constrained radio units.

The proposed framework demonstrates clear benefits for 6G-ready positioning, achieving over 90% sub-meter accuracy while reducing training time by approximately 45% through federated learning and pruning. These results highlight its suitability for dense, privacy-sensitive deployments, where distributed inference and lightweight models are essential. Overall, the combination of CSI-based RF fingerprinting, FL, and model compression provides a compelling solution for future 6G indoor navigation, industrial automation, and secure localization services. Future work could explore the integration of Reconfigurable Intelligent Surfaces (RISs) to further enhance CSI-based localization, particularly in challenging industrial or dense indoor environments.

Author Contributions: Conceptualization, I.A.B. and A.K.P.; methodology, I.A.B., A.K.P., D.I.K. and I.S.V.; software, I.A.B. and M.-L.A.B.; validation, I.A.B., M.-L.A.B. and A.K.P.; formal analysis, M.-L.A.B. and A.K.P.; investigation, M.-L.A.B. and A.K.P.; resources, I.A.B., A.K.P., D.I.K. and I.S.V.; writing—original draft preparation, I.A.B.; writing—review and editing, I.A.B., M.-L.A.B. and A.K.P.; visualization, I.A.B. and M.-L.A.B.; supervision, A.K.P., D.I.K. and I.S.V.; project administration, D.I.K. and I.S.V. All authors have read and agreed to the published version of the manuscript.

Funding: This research received no external funding.

Data Availability Statement: Data are available upon request from the authors.

Conflicts of Interest: The authors declare no conflicts of interest.

Abbreviation

Abbreviation	Definition
3GPP	Third Generation Partnership Project
AI	Artificial Intelligence
ADCPM	Angle–Delay Channel Power Matrix
BBK	Bayesian Bright Knowledge
BNN	Bayesian Neural Network
CIR	Channel Impulse Response
CNN	Convolutional Neural Network
CSI	Channel State Information

DoA	Direction-of-Arrival
FL	Federated Learning
GPS	Global Positioning System
JADE	Joint Angle and Delay Estimation
LOS	Line of Sight
MIMO	Multiple-Input Multiple-Output
mmWave	Millimeter Wave
NLoS	Non-Line-of-Sight
QoS	Quality of Service
RMSE	Root-Mean-Square Error
RSSI	Received Signal Strength Indicator
SRS	Sounding Reference Signals
TOA	Time of Arrival
TDoA	Time Difference of Arrival
UE	User Equipment
UMi	Urban Microcell

References

1. Bartsiokas, I.; Gkonis, P.; Kaklamani, D.; Venieris, I. ML-Based Radio Resource Management in 5G and Beyond Networks: A Survey. *IEEE Access* **2022**, *10*, 83507–83528. [CrossRef]
2. Bartsiokas, I.A.; Avdikos, G.K.; Lyridis, D.V. Deep Learning-Based Beam Selection in RIS-Aided Maritime Next-Generation Networks with Application in Autonomous Vessel Mooring. *J. Mar. Sci. Eng.* **2025**, *13*, 754. [CrossRef]
3. Behravan, A.; Yajnanarayana, V.; Keskin, M.F.; Chen, H.; Shrestha, D.; Abrudan, T.E.; Svensson, T.; Schindhelm, K.; Wolfgang, A.; Lindberg, S.; et al. Positioning and sensing in 6G: Gaps, challenges, and opportunities. *IEEE Veh. Technol. Mag.* **2023**, *18*, 40–48. [CrossRef]
4. Mogyorósi, F.; Revisnyei, P.; Pašić, A.; Papp, Z.; Törös, I.; Varga, P.; Pašić, A. Positioning in 5G and 6G Networks—A Survey. *Sensors* **2022**, *22*, 4757. [CrossRef] [PubMed]
5. Lu, Y.; Richter, P.; Lohan, E.S. Opportunities and Challenges in the Industrial Internet of Things based on 5G Positioning. In Proceedings of the 2018 8th International Conference on Localization and GNSS (ICL-GNSS), Guimaraes, Portugal, 26–28 June 2018; IEEE: Piscataway, NJ, USA, 2018; pp. 1–6.
6. Tariq, Z.B.; Cheema, D.M.; Kamran, M.Z.; Naqvi, I.H. Non-GPS positioning systems: A survey. *ACM Comput. Surv. (CSUR)* **2017**, *50*, 57. [CrossRef]
7. Brena, R.F.; García-Vázquez, J.P.; Galván-Tejada, C.E.; Muñoz-Rodriguez, D.; Vargas-Rosales, C.; Fangmeyer, J. Evolution of indoor positioning technologies: A survey. *J. Sens.* **2017**, *2017*, 2630413. [CrossRef]
8. Kulkarni, S.; Thakur, A.; Soni, S.; Hiwale, A.; Belsare, M.H.; Raj, A.B. A comprehensive review of direction of arrival (DoA) estimation techniques and algorithms. *J. Electron. Electr. Eng.* **2025**, *4*, 138–186. [CrossRef]
9. Saleh, S.; Sorour, S.; Noureldin, A. Vehicular positioning using mmWave TDOA with a dynamically tuned covariance matrix. In Proceedings of the 2021 IEEE Globecom Workshops (GC Wkshps), Madrid, Spain, 7–11 December 2021; pp. 1–6. [CrossRef]
10. Rathnayake, R.M.M.R.; Maduranga, M.W.P.; Tilwari, V.; Dissanayake, M.B. RSSI and Machine Learning-Based Indoor Localization Systems for Smart Cities. *Eng* **2023**, *4*, 1468–1494. [CrossRef]
11. Chen, H.; Keskin, M.F.; Aghdam, S.R.; Kim, H.; Lindberg, S.; Wolfgang, A.; Abrudan, T.E.; Eriksson, T.; Wymeersch, H. Modeling and analysis of OFDM-based 5G/6G localization under hardware impairments. *IEEE Trans. Wirel. Commun.* **2023**, *23*, 7319–7333. [CrossRef]
12. Liu, Q.; Gao, C.; Shang, R.; Gao, W.; López-Salcedo, J.A.; Seco-Granados, G. Hybrid GNSS+ 5G position and rotation estimation algorithm based on TOA and unit vector of arrival in urban environment. *IEEE Trans. Instrum. Meas.* **2024**, *73*, 9512908. [CrossRef]
13. Edjekouane, I.; Garrido, A.G.; Querol, J.; Chatzinotas, S. User Equivalent Range Error and Positioning Accuracy Analysis for ToA-Based Techniques Using PRS and SSB in 5G/6G NTN. *IEEE Open J. Commun. Soc.* **2025**, *6*, 9052–9072. [CrossRef]
14. Sharma, S.; Popli, R.; Singh, S.; Chhabra, G.; Saini, G.S.; Singh, M.; Sandhu, A.; Sharma, A.; Kumar, R. The Role of 6G Technologies in Advancing Smart City Applications: Opportunities and Challenges. *Sustainability* **2024**, *16*, 7039. [CrossRef]
15. Yang, Y.; Chen, M.; Blankenship, Y.; Lee, J.; Ghassemlooy, Z.; Cheng, J.; Mao, S. Positioning using wireless networks: Applications, recent progress and future challenges. *IEEE J. Sel. Areas Commun.* **2024**, *42*, 2149–2178. [CrossRef]
16. Li, P.; Fan, J.; Wu, J. Exploring the key technologies and applications of 6G wireless communication network. *iScience* **2025**, *28*, 112281. [CrossRef]

17. Alnoman, A.; Khwaja, A.S.; Anpalagan, A.; Woungang, A. Emerging AI and 6G-Based User Localization Technologies for Emergencies and Disasters. *IEEE Access* **2024**, *12*, 197877–197906. [CrossRef]
18. Ayaz, H.; Abbas, G.; Waqas, M.; Abbas, Z.H.; Bilal, M.; Nauman, A.; Jamshed, M.A. Physical layer security analysis using radio frequency-fingerprinting incellular-V2X for 6G communication. *IET Signal Process* **2023**, *17*, 5. [CrossRef]
19. Rother, B.; Kalis, N.; Haubelt, C.; Golatowski, F. Localization in 6G: A Journey along existing Wireless Communication Technologies. In Proceedings of the 2024 IEEE 20th International Conference on Factory Communication Systems (WFCS), Toulouse, France, 17–19 April 2024; pp. 1–7. [CrossRef]
20. Wu, Y.; Wang, Y.; Huang, J.; Wang, C.-X.; Huang, C. A Weighted Random Forest Based Positioning Algorithm for 6G Indoor Communications. In Proceedings of the 2022 IEEE 96th Vehicular Technology Conference (VTC2022-Fall), London, UK, 26–29 September 2022; pp. 1–6. [CrossRef]
21. Jagannath, A.; Jagannath, J.; Kumar, P.S.P.V. A comprehensive survey on radio frequency (RF) fingerprinting: Traditional approaches, deep learning, and open challenges. *Comput. Netw.* **2022**, *219*, 109455. [CrossRef]
22. Chen, R.; Liu, M.; Hui, Y.; Cheng, N.; Li, J. Reconfigurable Intelligent Surfaces for 6G IoT Wireless Positioning: A Contemporary Survey. *IEEE Internet Things J.* **2022**, *9*, 23570–23582. [CrossRef]
23. de Lima, C.; Belot, D.; Berkvens, R.; Bourdoux, A.; Dardari, A.; Guillaud, M.; Isomursu, M.; Lohan, E.-S.; Miao, Y.; Barreto, A.N.; et al. *6G White Paper on Localization and Sensing*; 6G Research Visions 2022, 12; University of Oulu: Oulu, Finland, 2022; Available online: http://urn.fi/urn:isbn:9789526226743 (accessed on 11 December 2025).
24. Meng, F.; Liu, S.; Gao, S.; Yu, Y.; Zhang, C.; Huang, Y.; Lu, Z. TDoA positioning with data-driven LoS inference in mmWave MIMO communications. *Signal Process.* **2024**, *220*, 109447. [CrossRef]
25. Pan, M.; Liu, P.; Liu, S.; Qi, W.; Huang, Y.; You, X.; Jia, X.; Li, X. Efficient joint DOA and TOA estimation for indoor positioning with 5G picocell base stations. *IEEE Trans. Instrum. Meas.* **2022**, *71*, 8005219. [CrossRef]
26. Morselli, F.; Razavi, S.M.; Win, M.Z.; Conti, A. Soft information-based localization for 5G networks and beyond. *IEEE Trans. Wirel. Commun.* **2023**, *22*, 9923–9938. [CrossRef]
27. Tedeschini, B.C.; Kwon, G.; Nicoli, M.; Win, M.Z. Real-Time Bayesian Neural Networks for 6G Cooperative Positioning and Tracking. *IEEE J. Sel. Areas Commun.* **2024**, *42*, 2322–2338. [CrossRef]
28. Cho, H.J.; Ahn, Y.; Shim, B. Transformer-Aided Mobile Positioning for 6G Ultra-Dense Networks. *IEEE Trans. Veh. Technol.* **2025**, *74*, 6839–6843. [CrossRef]
29. Tedeschini, B.C.; Kwon, G.; Nicoli, M.; Win, M.Z. Empowering 6G Positioning and Tracking with Bayesian Neural Networks. In Proceedings of the ICC 2024—IEEE International Conference on Communications, Denver, CO, USA, 9–13 June 2024; pp. 2276–2281. [CrossRef]
30. Yu, H.; Liu, Y.; Chen, M. Complex-Valued Neural-Network-Based Federated Learning for Multiuser Indoor Positioning Performance Optimization. *IEEE Internet Things J.* **2024**, *11*, 34065–34077. [CrossRef]
31. Zuo, Y.; Gui, L.; Cui, K.; Guo, J.; Xiao, F.; Jin, S. Mobile Blockchain-Enabled Secure and Efficient Information Management for Indoor Positioning with Federated Learning. *IEEE Trans. Mob. Comput.* **2024**, *23*, 12176–12194. [CrossRef]
32. Bartsiokas, I.A.; Gkonis, P.K.; Kaklamani, D.I.; Venieris, I.S. A Federated Learning-Based Resource Allocation Scheme for Relaying-Assisted Communications in Multicellular Next Generation Network Topologies. *Electronics* **2024**, *13*, 390. [CrossRef]
33. Bhattacharya, A.; Kumar, A. A shortest path tree based algorithm for relay placement in a wireless sensor network and its performance analysis. *Comput. Netw.* **2014**, *71*, 48–62. [CrossRef]
34. Study on Channel Model for Frequencies from 0.5 to 100 GHz, Document 3GPP TR 38.901, Release 17, 2023. Available online: https://www.google.com/url?sa=t&source=web&rct=j&opi=89978449&url=https://www.etsi.org/deliver/etsi_tr/138900_138999/138901/17.00.00_60/tr_138901v170000p.pdf&ved=2ahUKEwiQy4zax8ORAxVbyDgGHUZqJU0QFnoECBgQAQ&usg=AOvVaw2h8F-OKbNRJHZUxSZpSsPW (accessed on 11 December 2025).
35. 5G NR Physical Channels and Modulation, Document 3GPP TS 138 211, Version 15.3.0, Release 17, 2023. Available online: https://www.google.com/url?sa=t&source=web&rct=j&opi=89978449&url=https://www.etsi.org/deliver/etsi_ts/138200_138299/138211/15.03.00_60/ts_138211v150300p.pdf&ved=2ahUKEwjOydqsyMORAxXtxjgGHZw5Kf4QFnoECBkQAQ&usg=AOvVaw3WzegSSeBY_fr3xhF_kA5r (accessed on 11 December 2025).